10.1109/TIA.2023.3287817

An ElectroThermal Digital Twin for Design and Management of Radiation Heating in Industrial Processes

Enrico Spateri, Fredy Ruiz *Senior Member, IEEE,* and Giambattista Gruosso *Senior Member, IEEE*

***Abstract*—The design and management of thermoforming systems based on radiation heat transfer require the development of a mathematical model that can be used at all stages of the system's life cycle. For this reason, in this paper, we present a digital twin based on a hybrid ElectroThermal model that can integrate mathematical equations and data acquired in the field. The model's validity is verified with experiments performed on a test bench. The presented model is modular and can be easily used to represent new configurations of the heating elements for simulation and design. Thanks to the low computational complexity of the proposed Digital Twin, it enables the development of advanced control strategies and the analysis and optimization of the main geometric parameters of the system. In addition, it can support the identification of the best configuration and choice of measurement points.**

***Index Terms*—Digital Twins, ElectroThermal, Thermoforming, Heating Systems, Simulation, Mathematical Model**

I. Introduction

Thermoforming is a heat-assisted manufacturing process [1], [2] that involves heating, shaping, and cooling a sheet of polymer composite materials to obtain finished products with the desired shape and properties. The process can be schematized as follows: the sheet is loaded onto a frame and moved by a trolley system. It is heated directly, for example, by thermoelectric radiation technology (ceramic, quartz, or halogen heaters) and then shaped in pressure or vacuum molds. Depending on the desired profiles after molding, each machine consists of several heaters spatially arranged most suitably. Each of these heating elements represents a degree of freedom in the overall temperature control of the system. The key to successful sheet forming is an excellent definition of the temperature reference map. Temperatures that are too high cause excessive softening and thin or defective thermoforming layers, while temperatures that are too low cause excessive sheet stiffness and, consequently, cracks and surface defects in the product. Typically this adjustment is not trivial since the transit time of the sheet under the heater is another very important process variable. Since the thickness of the part depends drastically on the internal temperature distribution, it becomes essential to have a mathematical model that allows to obtain the optimal temperature mapping for the product being processed.

In literature, there are several approaches to obtaining a mathematical model for the heating process. The work described in [3] proposes a circuit model for describing the heater that is particularly efficient for defining fast analyses. In [4], modeling of the heater is provided using radiation equations through finite element software. Other approaches are based on a model of the slab obtained through numerical methods to the differential equations [5]. Of particular interest are the works [6], [7] in which the temperature dependence of material parameters is used to obtain a better prediction of the slab temperature. In contrast, [8] presents a geometric analytical model for determining the view factor in closed convection furnaces.

The main challenge in thermoforming processes remains the prediction of temperature distribution and the optimization of heating element parameters and their arrangement. This process can be conducted by trial and error or by a workflow based on empirical testing, as proposed in [9], [10].

The objective of this paper is to create a Digital Twin (DT) [11], [12] of the preheating and heating phases of the thermoforming process, to be used in the realization of an efficient control system.

The digital twin approach has many advantages: it allows hybrid models to be created based on simulations and collected data. These models can be used in both the design and operation phases to monitor proposed solutions continuously. They can also be used to build black-box models, easily embedded into on-board controllers.

Some digital twins for thermoforming processes have been proposed; see [13]–[17]. In each previous paper, the authors have focused on different aspects concerning the regulation and optimal placement of heating elements. Our original approach is intended to differ from the previous ones in that it is characterized as an inverse problem. Knowing the effects of the measurements on the slab, we determine the model's parameters inversely and thus have a relationship linking the input setpoint with the temperature distribution of the sheet surface. And this is done in a hybrid manner: the parts for which it is possible to model based on physical equations are treated mathematically, and those of more complex definitions are obtained in a data-driven manner. The method proposed in this article is innovative and aims to:

- Propose a hybrid model based on lumped-parameter elements, finite differences and experimental data for the description and analysis of the thermoforming phenomenon;
- Use data analysis techniques for the reconstruction of key coefficients of the radiation heat transfer phenomenon;

The authors are with Politecnico di Milano, Dipartimento di Elettronica Informazione e Bioingegneria, Piazza Leonardo da Vinci 32, 20133 Milano email: giambattista.gruosso@polimi.it.

- Verify with a laboratory setup the results obtained by the digital twin.

Numerical methods hybridized with data are often more flexible than purely analytical models for the representation of complex multi-physical systems due to a less physical lumped parametrization. These parameters can be highly variable during the thermoforming process due to the presence of mechanical, thermal, and fluid dynamics. Analytical models are highly dependent on external conditions and are usually avoided for their physical interpretation.
The hybrid model, integrating lumped parameters and finite differences technique, can be described by a large set of simple ODEs. Many toolboxes can solve them efficiently, allowing the usage of the hybrid model for the possible implementation and supervision of a real thermoforming machine. The developed model manages more than 100.000 elements. Data-driven integration allows for a better system description of different conditions by initial tuning (of heaters and power distribution parameters) and a future promising online updating. The use of non-data-driven model as investigated in [18] , and from the comparison with the proposed methodology are clear advantages.

The paper is organized as follows: in section II the thermal-radiative model is explained. In section III, the heater structure, I/O diagram and test bench configuration are presented, combined with the experimental measurement. In the conclusion section IV, the main results and future work are highlighted.

II. Methodology and Mathematical Model

Managing thermoformed products' specifications and production yield requires a good choice of fundamental process parameters. The most delicate set of operating parameters concerns the management of heating power applied to each element. Each heating core is heated through Joule dissipation of the internal resistor winding. Then, the heaters transfer heat to the sheet by irradiation, which is a surface-to-surface exchange phenomenon that does not lead to a homogeneous temperature distribution across the thickness of the sheet.

As shown in Fig. 1, during the heating phase of the sheet, the temperatures of the bulk (T_{bulk}) and of the surface ($T_{surface}$) have different time transients. The surface is heated directly, so its transient is faster than the dynamics of the bulk temperature. However, a polymer composite can be molded when both bulk and surface temperatures are in the thermoforming range. It is necessary to analyze the optimal set of parameters for the heating elements to bring the sheet temperature to the thermoforming range in the minimum heating time.

The heating phase in the thermoforming process can be represented as a dynamic system organized into three distinct phases: the generation of heat from electric power within the heating elements, power transmission as radiation heat through air from the heating elements to the polymer sheet, and the diffusion of heat into the sheet. These three phenomena are closely connected through inputs and outputs but can be regarded as independent. In the proposed model, described in Fig. 2, the three blocks constitute the hybrid digital twin are defined as :

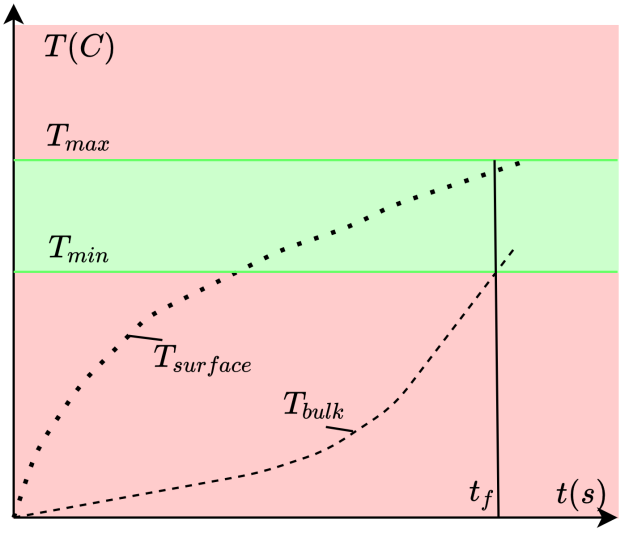

Fig. 1. The Thermal Transient on the Surface and in the Bulk are different and there is a delay. The optimal thermoforming is obtained when the two temperatures are both in the green region.

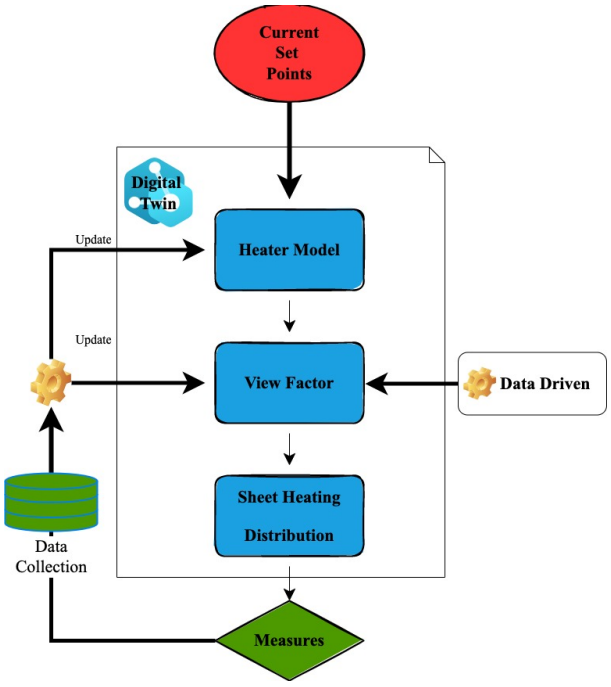

Fig. 2. Flowchart of the Digital Twin implementation

- [A] Heat radiation physical model ;
- [B] Viev factor data-based model;
- [C] Diffusion Block physical model.

The main parameters involved in the three systems are described in Table I. In the following three sub-sections, the operating principle of each of the individual blocks is clarified.

A. Heater Model

Each heater element is modeled using a lumped parameters model describing a thermo-electric ceramic heater, as repre-

TABLE I
LEGEND FOR PARAMETERS AND UNITS

Heater		Sheet	
Symbol	Quantity	Symbol	Quantity
P_{in}	Heater input power	$T_{i,j}$	Sheet temperature
σ	Stefan-Boltzmann Const	c_{sheet}	specific heat
A_c	Heater surface area	h_{up-dw}	Air convection Const
ϵ	Adimensional emissivity	$T_{i,j}$	Sheet temp.
c_{pc}	Specific heat	ρ	Sheet density
V_c	Heater Volume	V	Sheet cell volume
ρ_c	Heater density	k	Conduction const.
h_{conv}	Air Convection coefficient	A	Surface element area
T_∞	Room temperature	Δz	Node thickness

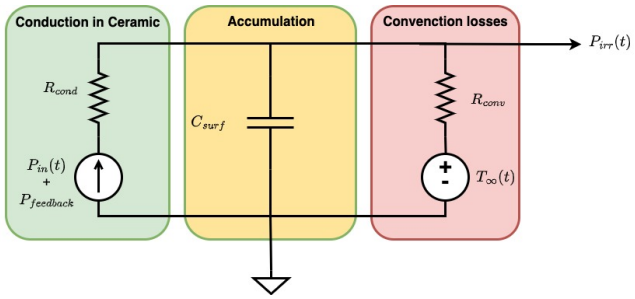

Fig. 3. The phenomenon can be represented using a lumped parameters circuit made by three contributions: the conduction in ceramic parts, the accumulation due to thermal inertia, and the convention losses.

sented in Fig. 3. The regulation of each heater current (we refer in the paper to the input conductive power $P_{in}(t)$ as Joule losses) allows a nonlinear radiation power generation described as follows:

$$P_{in}(t) = A_c\sigma\epsilon T^4_{surf}(t) + c_{pc}V_c\rho_c\frac{\delta T_{surf}(t)}{\delta t} + h_{conv}A_c(T_{surf}(t) - T_\infty) \quad (1)$$

The first right-hand term represents the total infrared radiation output with the Stefan-Boltzmann constant σ, the adimensional emissivity ϵ, and the heater surface area. The second term describes the heat storage term with the heater-specific heat c_h, the volume V_c, and the density ρ_c. The air convection heat transfer is represented by the last term described by the convection coefficient h_{conv} and evaluated with respect to the environment temperature T_∞.

To calibrate and validate the model, experimental analyses were performed on the heaters. A current capable of supplying 20% of the rated power for a sufficiently long time, compatible with the system's time constant, was applied to a single heater. Figure 4 compares the response measured by the internal temperature sensor, a NTC thermistor (solid line) and the predicted response (dashed line). The model describes the heater bulk temperature well for the upward phase. In contrast, for the downward transient the model is less accurate due to the contribution of convection, which is not considered in the proposed model. For the scope of the work, this phenomenon

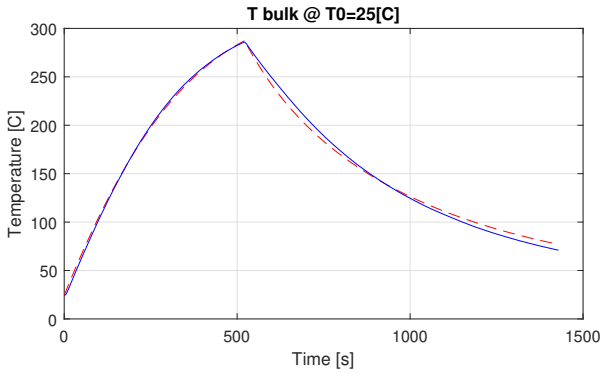

Fig. 4. The validation of heaters model has been obtained by means of an experimental setup. In this figure a comparison between measured temperatures (solid lines), and hybrid model results (dashed lines) is reported. To measure the bulk temperature we use an NTC sensor embedded by the manufacturer in the heating element

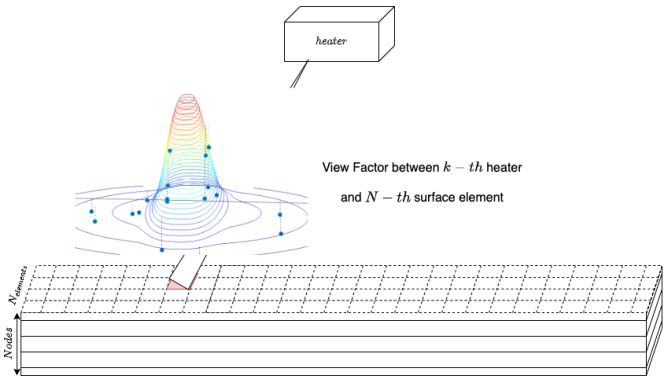

Fig. 5. The sheet is discretized through a surface mesh that is extruded along the thickness of the sheet. The view factor is calculated as a surface between the radiation point (the $k-th$ heater) and each of the N surface element

is, in fact, not of interest, assuming that we want to regulate only when current flows in the system.

B. View Factor Model

This element is modelled by conducting a series of experiments considering only one active heather at a time and measuring the temperature distribution on the sheet. From the set of measurements thus obtained, the model parameters are determined using a fitting operation as explained below.
The view factor (Z) relates the power radiated by each heater to the power flow arriving on the sheet surface. It is a parameter that maps the radiation heat emitted by each element to the power arriving to each point on the polymer sheet. To model this phenomenon, the temperature is considered to be uniform over the surface of the heater, and the surface of the sheet is assumed to be divided into several sub-elements of square shape, see Fig. 5. The bond between each heating element and each sub-element on the sheet's surface can be described by a matrix, named the View Factor. The view factor matrix can be calculated numerically using the heat propagation equations given the system geometry. Yet, there are many sources of uncertainty in the process, so a Data-Driven approach is proposed in this work. A set of

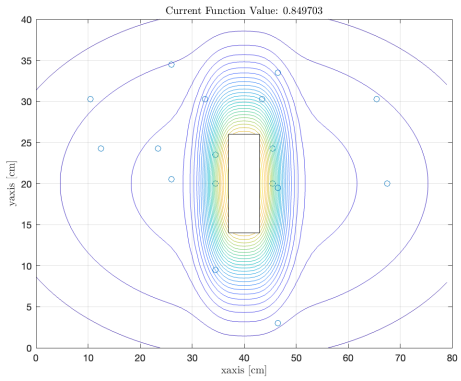

Fig. 6. Top View of the View factor surface obtained with the values $(\sigma_{x,heat} = 11.2, \sigma_{y,heat} = 23.2, \sigma_{x,back} = 1872, \sigma_{y,back} = 380, w_1 = 0.1, w_2 = 0.5)$. The cost function value is 0.849 [K/s].

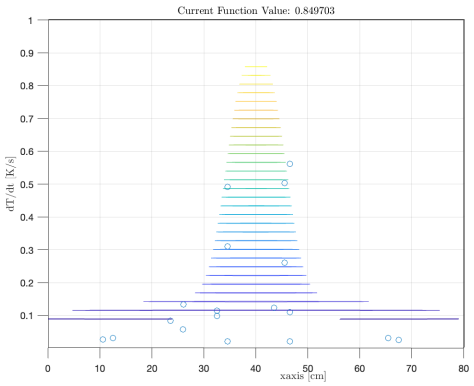

Fig. 7. Side View of the View factor surface obtained with the values $(\sigma_{x,heat} = 11.2, \sigma_{y,heat} = 23.2, \sigma_{x,back} = 1872, \sigma_{y,back} = 380, w_1 = 0.1, w_2 = 0.5)$. The cost function value is 0.849 [K/s].

measurements are made on a test bench: each heater is heated to its equilibrium temperature, then a sheet is inserted. The temperature on sheet's surface is measured by remote-sensing thermometers (pyrometers) mounted on the bench. For the sake of simplicity, we choose only 8 measurement points (4 in the upper layer and 4 in the bottom) that correspond to boundary points and central point.

The data map of the temperature derivatives is arranged according to the relative distance from the active heater (circles in Figs. 6 and 7). A constrained optimization problem based on the L_2 norm is defined to minimize the difference between the map of the temperature derivatives $\dot{T}_{obj}$ observed in the experiment and the temperature derivatives predicted by the model of the view factor and the sheet thermodynamics, at the initial experiment time $\dot{T}_s(0)$. The view factor function is parametrized as the superposition of two bivariate normal distributions weighted to consider the background radiation and the direct radiation of the heater. The view factor at a given point $x_{c,i}, y_{c,i}$ is calculated as the mean integral value of the normalized distributions superimposed on each sheet surface element given in eq. 2.

$$\begin{aligned} Z_i(x_{c,i}, y_{c,i}) = &\int_A \frac{w_1}{2A\pi\sigma_{x,h}\sigma_{y,h}(w_1+w_2)} \\ &exp(-\left[\frac{x_i - x_{c,i}}{\sqrt{2}\sigma_{x,h}}\right]^2 - \left[\frac{y_i - y_{c,i}}{\sqrt{2}\sigma_{y,h}}\right]^2)dA \\ &+ \int_A \frac{w_2}{2A\pi\sigma_{x,b}\sigma_{y,b}(w_1+w_2)} \\ &exp(-\left[\frac{x_i - x_{c,i}}{\sqrt{2}\sigma_{x,b}}\right]^2 - \left[\frac{y_i - y_{c,i}}{\sqrt{2}\sigma_{y,b}}\right]^2)dA \end{aligned} \tag{2}$$

The decision variables of the optimization problem are the parameters of the background distribution $(\sigma_{x,back}, \sigma_{y,back})$, the direct heating distribution $(\sigma_{x,heat}, \sigma_{y,heat})$ and the weights for the normalization of the two distributions (w_1, w_2), subject to the following constraints about the starting temperature and the upper and lower bounds of standard deviations and weights.

$$\begin{cases} \dot{T}_s(t_0) = \frac{2a}{A_{element}}\epsilon\sigma A_c T_{sat,res}^4 Z(x, y, \sigma_x, \sigma_y) \\ T_s(0) = T_{room} \\ 10 \leq \sigma_{x,heat} \leq 80 \quad 10 \leq \sigma_{y,heat} \leq 80 \\ 10 \leq \sigma_{x,back} \leq 8000 \quad 10 \leq \sigma_{y,back} \leq 8000 \\ 0.05 \leq w_1 \leq 1 \quad 0.01 \leq w_2 \leq 0.6 \end{cases} \tag{3}$$

The results of the optimization process are shown in Figs. 6 and 7.

C. Sheet Heating

The internal temperature distribution in the sheet is calculated by subdividing it along its thickness in layers called nodes, see Fig. 5. The temperature dynamic equations are based on the energy balance for the nodes of the sheet for each surface element of the grid. The energy balance on the top and bottom layers of the sheet for the generic i^{th} node, using a finite differences formulation, is expressed as:

$$\frac{dT_i}{dt} = \frac{1}{\rho V c_{sheet}}\left[P_{abs.i} + \frac{kA}{\Delta z}(T_{i-1} - T_i) - \frac{kA}{\Delta z}(T_i - T_{i+1})\right] \tag{4}$$

At the two boundaries, the equations become the following due to the imposition of the convection conditions:

$$\frac{dT_1}{dt} = \frac{1}{\rho V c_{sheet}}\left[P_{abs,1} - P_{conv,1} - \frac{kA}{\Delta z}(T_1 - T_2)\right] \tag{5}$$

$$\frac{dT_N}{dt} = \frac{1}{\rho V c_{sheet}}\left[P_{abs,N} + P_{conv,N} + \frac{kA}{\Delta z}(T_{N-1} - T_N)\right] \tag{6}$$

where $P_{conv,1}$ and $P_{conv,N}$ are the absolute power values exchanged by convection at layer 1 and N.

The state matrix obtained is a tridiagonal matrix representing the layer-by-layer conduction in its core and the convection power flow for the boundaries [15].

III. Experimental Result and Method Validation

For both the model creation and validation stages, a workbench representing a thermoforming machine in small scale

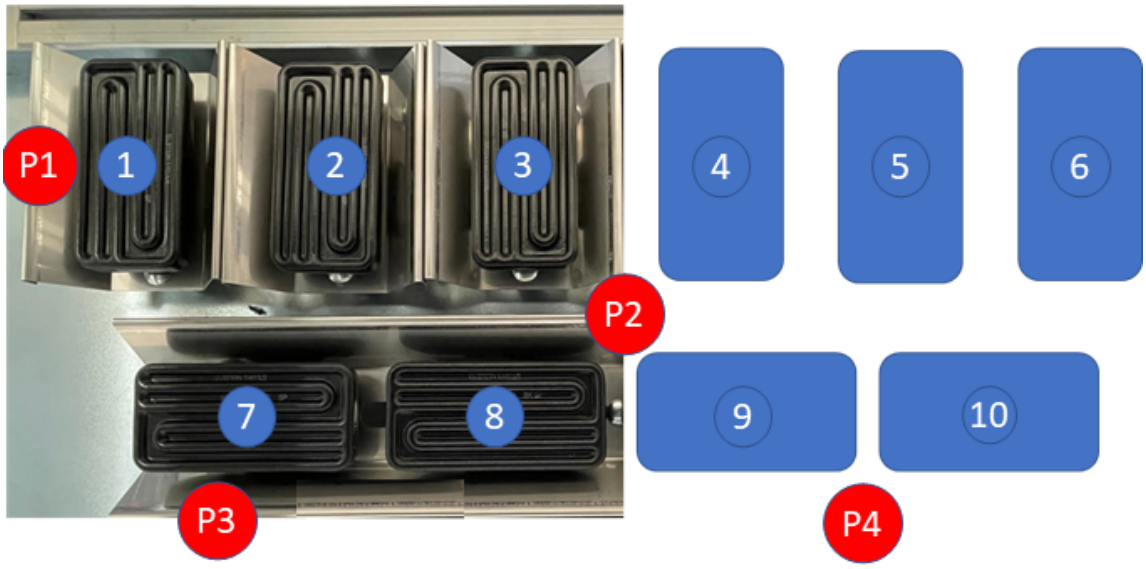

Fig. 8. Functional description of the Test Bench: the upper part and the lower part are equal and are made by 10 heating elements, disposed as reported in the figure.

was created. This machine consists of two radiating surfaces that can be set at different distances from the sheet plane. Each radiating surface consists of 10 ceramic heaters arranged as shown in Fig. 8. The power of each heater is $500W$.
On both sides of the stand, 4 pyrometers are symmetrically arranged for measuring the surface temperature of the slab (P1, P2, P3, and P4), positioned as shown in Fig. 8.

A. Heaters Model Validation

Several tests have been performed for the fitting of the model parameters and for the creation of the view factor matrix. One test is given as example, where only a subset of the heaters (4, 7, and 8 shown in Fig. 8) are turned on, and they are individually powered at 25% of their rated power. Figure 9 compares the result of the simulation of the proposed method (dashed) with the temperature measured by the NTC thermistors inside the heaters (solid lines). The predicted temperatures show a relative error of less than 10% at the steady-state temperature point with respect to the experimental measurements. The discrepancies are mainly due to the effect of external factors that cannot be easily reproduced.

The more the heater is placed in the center of the slab, the more the exchange with the environment is reduced, resulting in decreased power output and increased saturation temperature. The differences in the initial slope of the transient are caused by the disturbance of structural parameters and the arrangement of temperature sensors in the heater core. Due to the ceramic material layer of the heater, the surface temperature is slightly delayed by $2-5s$ from the measured internal temperature. A delay block might be added to the last input of the system for this purpose.

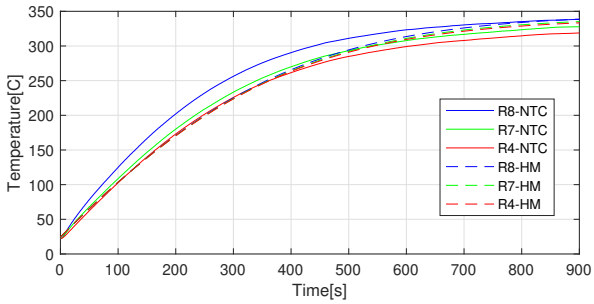

Fig. 9. Simulated (dashed) vs Measured (solid) Temperatures in three heaters

B. Complete Model Validation

In this subsection, we report an experiment (among several done) made on a polystyrene sheet 3.1[mm] thick. The slab, which is at an ambient temperature of about 30 degrees Celsius, is inserted when the heaters have already reached the equilibrium temperature. In this way, only the effect of the steady-state condition of the heaters on the sheet is measured. In the Figures 10, 11, 12 and 13, the most significant measurements of the pyrometers (dashed lines) are compared with the temperatures predicted by the hybrid model (solid lines) for a single heater turned on (heater 9 in Fig. 8) placed near the sensing point of pyrometers P2 and P4. For the other two measurement points (P1 and P3), the temperature is lower because of the larger distance to the active heaters.

In addition, the hybrid model predicts internal node temperatures (green for the mid-slab node) that cannot be measured in the experimental environment. It can be seen that the pyrometer measurements are in good agreement with the simulations. Table II shows the mean and maximum values of the absolute temperature error for each time step.

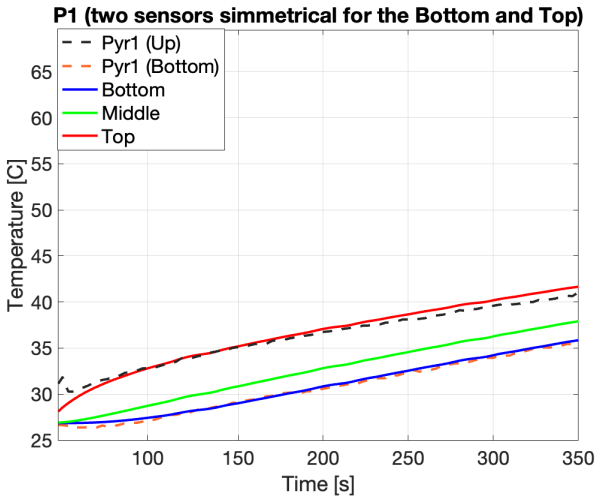

Fig. 10. (Figure reports the comparison between two measured temperatures in the point P1 (Fig. 8)) acquired by two pyrometers (in the top and the bottom of the sheet) compared with three simulation point (top, middle and bottom of the sheet)

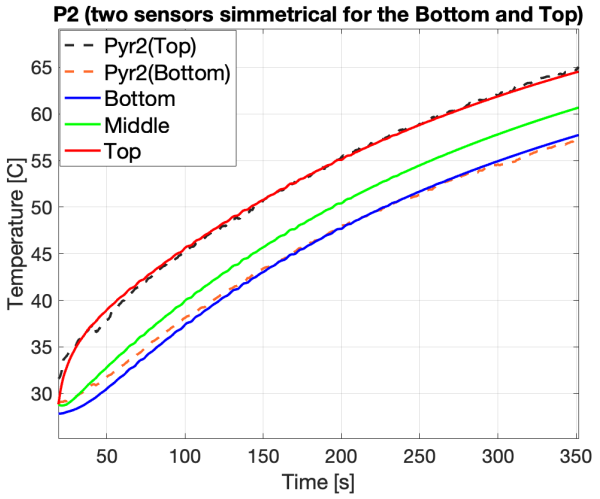

Fig. 11. Figure reports the comparison between two measured temperatures in the point P2 (Fig. 8) acquired by two pyrometers (in the top and the bottom of the sheet) compared with three simulation point (top, middle and bottom of the sheet)

Side	Pyrometer	**Max error [C]**	**Mean [C]**
Top	1-Up	3.45	1.07
	2-Up	7.16	0.93
	3-Up	3.58	1.68
	4-Up	3.96	6.26
Bottom	1-Dw	0.51	0.67
	2-Dw	3.55	5.36
	3-Dw	1.78	1.05
	4-Dw	3.56	6.03

TABLE II
MEAN AND MAXIMUM ABSOLUTE ERRORS FOR TOP AND BOTTOM OF THE SHEET FOR THE PROPOSED MODEL COMPARED TO ALL THE SYMMETRIC PYROMETER MEASUREMENTS.

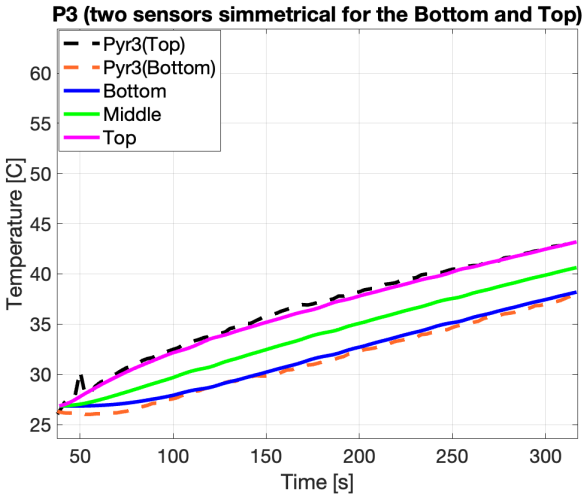

Fig. 12. Figure compares two measured temperatures in point P3 (Fig. 8 acquired by two pyrometers (in the top and the bottom of the sheet) compared with three simulation points (top, middle, and bottom of the sheet)

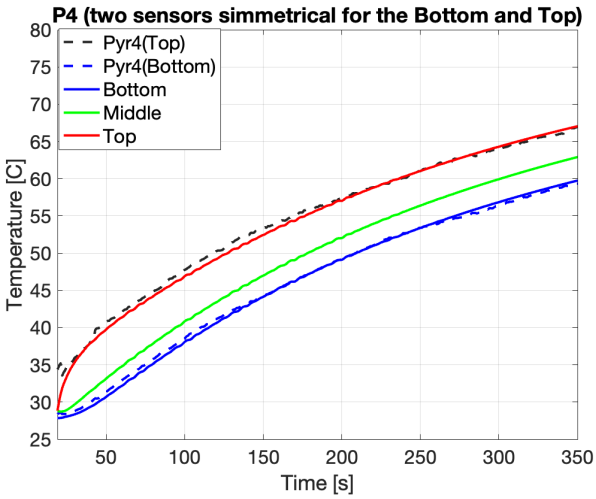

Fig. 13. Upper (Figure reports the comparison between two measured temperatures in the point P4 (Fig. 8) acquired by two pyrometers (in the top and the bottom of the sheet) compared with three simulation points (top, middle, and bottom of the sheet)

C. *Surface distribution tests*

The digital twin proposed in this paper is tested by imposing four different input power profiles. Fig. 14 shows the predicted temperatures on the top surface of the slab as obtained from the simulations. The blue dots represent the position of the pyrometers used for the measurement. The central part was discretized with square elements of $5 \times 5\ cm^2$. A homogeneous distribution of temperatures is obtained in Test I. In Test II, horizontal temperature bands are imposed. In Test III, the temperature is set in bands arranged on the corners. In Test IV, on the other hand, the temperature is set higher on the center of the sheet. The results of the four configurations were compared with the behavior of the test bench. The heaters were brought to equilibrium temperatures, and then the sheet was inserted. Table III shows the predicted and measured temperature increments measured on the top surface.

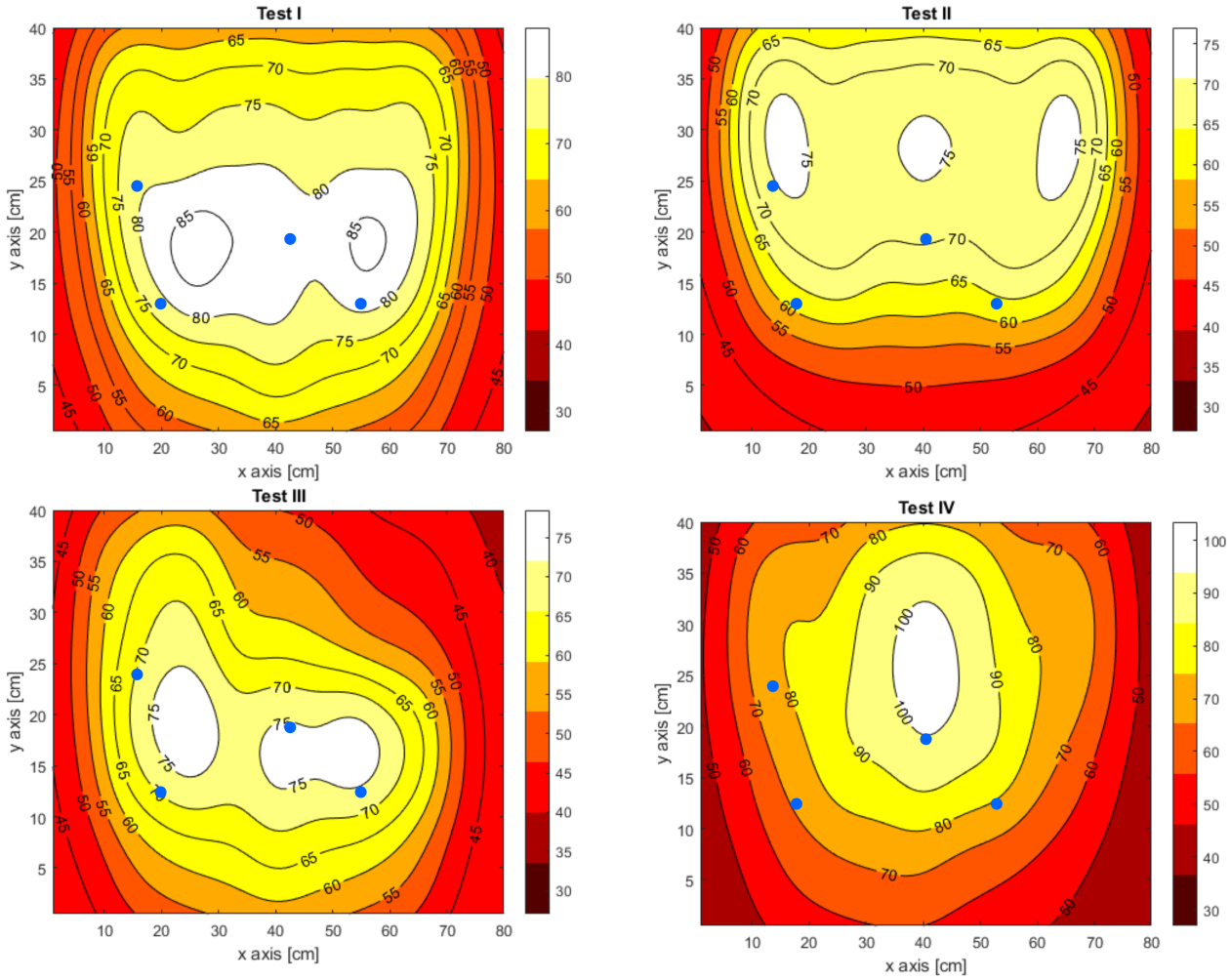

Fig. 14. Sheet measured temperatures [C] of the Top of the sheet obtained by imposing a temperature set-point after $20s$ compared with the simulation in 4 cases

TABLE III
COMPARISON BETWEEN SIMULATED ($T_{sheet}(t_f) - T(0)$) AND MEASURED TEMPERATURE IN THE TEST

	Test I		Test II	
Pyr	Simulated [C]	Measured [C]	Simulated [C]	Measured [C]
1	79	78	74	75
2	83	83	72	73
3	78	81	63	57
4	82	81	63	57
	Test III		Test IV	
Pyr	Simulated [C]	Measured [C]	Simulated[C]	Measured [C]
1	72	75	82	84
2	76	74	104	96
3	71	68	76	75
4	75	71	78	77

IV. CONCLUSION

A hybrid (data- and model-based) digital twin for the dynamics of an irradiation-based thermoforming process is described, analyzed and validated step by step with data measured on a test bench. The main parameters involved were phased through measurements made on the bench and compared with those in the literature. Each module of the hybrid model was validated with experimental measurements. Then, the model was validated for four temperature distributions, verified against measurements. The four different operating settings, compared with the temperatures predicted by the hybrid model, highlight the efficiency of this application for non-softening regions. Future uses of this model will involve the development of advanced optimization algorithms for heating power supply, control strategy studies, and reorganizing heating banks with optimized geometries.

REFERENCES

[1] G. Gruenwald, *Thermoforming: A Plastics Processing Guide,*, 2nd ed. New York: Routledge, 2017.
[2] J. Throne, *Technology of thermoforming*, 1st ed. Munich: Hanser, 1996.
[3] P. Girard and V. Thomson, "Energy model based control for forming processes," pp. 1–9, 2008, collection / Collection : NRC Publications Archive / Archives des publications du CNRC.
[4] F. Schmidt, Y. Le Maoult, and S. Monteix, "Modelling of infrared heating of thermoplastic sheet used in thermoforming process," *Journal of Materials Processing Technology*, vol. 143-144, pp. 225–231, 2003, proceedings of the International Conference on the Advanced Materials Processing Technology, 2001.

[5] G. Gauthier, M. Ajersch, B. Boulet, A. Haurani, P. Girard, and R. DiRaddo, "A new absorption based model for sheet reheat in thermoforming," pp. 353–357, May 2005, collection / Collection : NRC Publications Archive / Archives des publications du CNRC.

[6] S. A. Khan, P. Girard, N. Bhuiyan, and V. Thomson, "Improved mathematical modeling for the sheet reheat phase during thermoforming," *Polymer Engineering and Science*, vol. 52, no. 3, p. 625 – 636, 2012.

[7] A. Yousefi, A. Bendada, and R. Diraddo, "Improved modeling for the reheat phase in thermoforming through an uncertainty treatment of the key parameters," *Polymer Engineering and Science*, vol. 42, no. 5, p. 1115 – 1129, 2002.

[8] M. I. Chy and B. Boulet, "Development of an improved mathematical model of the heating phase of thermoforming process," in *2011 IEEE Industry Applications Society Annual Meeting*, 2011, pp. 1–8.

[9] B. Buffel, B. van Mieghem, A. van Bael, and F. Desplentere, "A combined experimental and modelling approach towards an optimized heating strategy in thermoforming of thermoplastics sheets," *International Polymer Processing*, vol. 32, no. 3, pp. 378–386, 2017.

[10] B. Buffel and F. Desplentere, "A combined experimental and numerical study on pulsed heating of thermoplastic sheets in thermoforming," vol. 2139, 2019.

[11] D. Hartmann and H. Van der Auweraer, "Digital twins," in *Progress in Industrial Mathematics: Success Stories*, M. Cruz, C. Parés, and P. Quintela, Eds. Cham: Springer International Publishing, 2021, pp. 3–17.

[12] C. Cimino, G. Ferretti, and A. Leva, "The role of dynamics in digital twins and its problem-tailored representation," *IFAC-PapersOnLine*, vol. 53, no. 2, pp. 10 556–10 561, 2020, 21st IFAC World Congress.

[13] R. Modirnia and B. Boulet, "Model-based virtual sensors and core-temperature observers in thermoforming applications," *IEEE Transactions on Industry Applications*, vol. 49, no. 2, pp. 721–730, 2013.

[14] A. Hürkamp, R. Lorenz, T. Ossowski, B.-A. Behrens, and K. Dröder, "Simulation-based digital twin for the manufacturing of thermoplastic composites," *Procedia CIRP*, vol. 100, pp. 1–6, 2021, 31st CIRP Design Conference 2021 (CIRP Design 2021).

[15] E. Spateri, F. Ruiz, and G. Gruosso, "Modelling and analysis of radiation heating in thermoforming processes," in *2022 IEEE 21st Mediterranean Electrotechnical Conference (MELECON)*, 2022, pp. 249–254.

[16] E. Turan, Y. Konuşkan, N. Yıldırım, D. Tunçalp, M. İnan, O. Yasin, B. Turan, and V. Kerimoğlu, "Digital twin modelling for optimizing the material consumption: A case study on sustainability improvement of thermoforming process," *Sustainable Computing: Informatics and Systems*, vol. 35, p. 100655, 2022.

[17] F. Erchiqui, H. Kaddami, G. Dituba-Ngoma, and F. Slaoui-Hasnaoui, "Comparative study of the use of infrared and microwave heating modes for the thermoforming of wood-plastic composite sheets," *International Journal of Heat and Mass Transfer*, vol. 158, p. 119996, 2020.

[18] E. Spateri, F. Ruiz, and G. Gruosso, "A Digital Twin for Analysis of Radiation Heating in Thermoforming Processes," vol. 2021-October, 2021.

V. Biography Section

Enrico Spateri Enrico Spateri was born in Milano (Italy). He received the Bachelor (2018) in Engineering Physics and the M.Sc. (2021) in Automation and control engineering both from Politecnico di Milano (Italy). He is actually a Ph.D. candidate in Electrical engineering. His research focuses on analysis, reduced order modeling and optimization for electro-thermal and electromagnetic-thermal coupled problems and applications including thermoforming, induction heating and induction thermography.

Fredy Ruiz Fredy Ruiz was born in Facatativa(Colombia). He received the Bachelor (2002) and M.Sc. (2006) degrees in Electronics Engineering, both from Pontificia Universidad Javeriana (Colombia), and the Ph.D. (2009) degree in Computer and Control Engineering from the Politecnico di Torino (Italy). Fredy was Assistant (2010-2014) and Associate (2015-2019) professor at Pontificia Universidad Javeriana(Colombia), where He also served as Head of the Electronics Engineering Department between 2014 and 2016. He was Fulbright visiting scholar at the University of California, Berkeley in 2013 and Visiting professor at the Politecnico di Torino in 2018. He is Currently Associate professor at Politecnico di Milano, Italy. His research activity focuses in control and optimization, in particular, the use and of data-driven techniques in optimal estimation and controller design, with applications in smart-grids, power electronics, robotics and bio-technology. He works also in the design of demand side management strategies for the smart-grid.

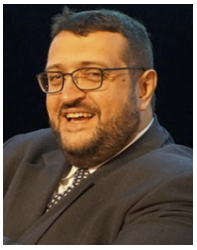

Giambattista Gruosso (Senior Member, IEEE) was born in 1973. He received the B.S. and M.S. degrees in electrical engineering and the Ph.D. degree in electrical engineering from the Politecnico di Torino, Italy, in 1999 and 2003, respectively. From 2002 to 2011, he was an Assistant Professor with the Department of Electronics and Informatics, Politecnico di Milano, where he has been an Associate Professor, since 2011. He is the author of more than 80 papers on Journals and conferences on the topics. He does research in electrical engineering, electronic engineering, and industrial engineering. His main research interests include electrical vehicles transportation electrification, electrical power systems optimization, simulation of electrical systems, digital twins for smart mobility, factory and city, and how they can be obtained from data. He is the head of Simlab40 group at Politecnico di Milano https://www.simlab40.deib.polimi.it